

The trispectrum in ghost inflation

Qing-Guo Huang *

Kavli Institute for Theoretical Physics China (KITPC), Key Laboratory of Frontiers in
Theoretical Physics, Institute of Theoretical Physics, Chinese Academy of Sciences,
Beijing 100190, China

ABSTRACT: We calculate the trispectrum in ghost inflation where both the contact diagram and scale-exchange diagram are taken into account. The shape of trispectrum is discussed carefully and we find that the local form is absent in ghost inflation. In general, for the non-local shape trispectrum there are not analogous parameters to $\tau_{NL}^{loc.}$ and $g_{NL}^{loc.}$ which can completely characterize the size of local form trispectrum.

KEYWORDS: inflation, non-gaussianity.

*huangqg@itp.ac.cn

Contents

1. Introduction	1
2. The Hamiltonian density in the interaction picture	3
3. The power spectrum	4
4. The trispectrum	5
4.1 Contact diagram	8
4.2 Scalar-exchange diagram	11
5. Discussions	16

1. Introduction

Even though inflation is an elegant paradigm in the early universe, a realistic inflation model is still not known. A near scale-invariant primordial power spectrum can be taken as one of the predictions of inflation. Nowadays the three-point and four-point correlation functions of the curvature perturbations, so-called bispectrum and trispectrum, have been a sensitive probe of the physics in the early universe. These correlation functions encode rich information about the detail of inflation and may help us to understand the physics in the early universe.

For simplicity, we classify the bispectrum and trispectrum to be local and non-local shapes [1]. A large local-shape non-Gaussianity can be generated at the end of inflation [2, 3, 4, 5] due to the non-trivial condition for multi-field inflation to end, or deep in the radiation era [6, 7, 8, 9, 10, 11, 12]. See other relevant papers in [13]. In general the multi fields must be involved in order to generate large local-shape bispectrum and trispectrum. The local-shape non-Gaussianity is much more sensitive to the experiments. WMAP 7yr data [14] implies $-10 < f_{NL}^{loc} < 74$ at 95% C.L.. A convincing detection of such a large local-shape non-Gaussianity will rule out all single-field inflation models.

However a large non-local form non-Gaussianity is also allowed by WMAP 7yr data [14, 15]. The mechanism for producing a non-local form non-Gaussianity is quite different from a local form non-Gaussianity. The non-local form non-Gaussianity is generated on the horizon scale during inflation, and all of the relevant perturbation modes have roughly the same wavelength. In general, higher derivative terms in the action of the inflaton field are called for in order to produce a large non-local form bispectrum and trispectrum. The mixed scenario in [15] opens a window to achieve not only local form but non-local form non-Gaussianity in one model where the higher derivative terms for the inflaton along

the adiabatic direction contributes to a large non-local shape non-Gaussianity, and the other light scalar fields, such as curvaton(s), produce a large local shape non-Gaussianity. A distinguishing phenomenology for the mixed scenario is that $\tau_{NL}^{loc.}$ must be larger than $(\frac{6}{5}f_{NL}^{loc.})^2$.

In this paper we focus on the primordial trispectrum in the ghost inflation model [16] based on the idea of ghost condensate [17]. We will see that the local shape trispectrum is absent in this single field model. The ghost condensate is a new kind of fluid that can fill the universe. It has the equation of state $p = -\rho$ and provides an alternative way of realizing de Sitter phases in the early universe. The ghost scalar field ϕ condenses in a background where it has a non-zero velocity

$$\langle \dot{\phi} \rangle = M^2, \quad (1.1)$$

where M is the ghost cur-off scale and the scalar field ϕ has a constant velocity $\langle \dot{\phi} \rangle$ from ghost condensation. Several observational constraints on the cut-off scale, for example $M < 100$ GeV, are discussed in [16, 17]. The ghost condensate is not a cosmological constant, it is a physical fluid with a physical scalar excitation Q defined as

$$\phi = M^2 t + Q. \quad (1.2)$$

Assuming that the ghost field ϕ has a shift symmetry $\phi \rightarrow \phi + \delta$, we conclude that the ghost field must be derivatively coupled. Based on the symmetry of this theory, we construct the action for Q as follows

$$S = \int d^4x \sqrt{-g} \left[\frac{1}{2} \dot{Q}^2 - \frac{\alpha^2}{2M^2} (\nabla^2 Q)^2 + \mathcal{L}_{int}^{(3)} + \mathcal{L}_{int}^{(4)} + \dots \right], \quad (1.3)$$

where

$$\mathcal{L}_{int}^{(3)} = -\frac{\beta_1}{2M^2} \dot{Q} (\nabla Q)^2 - \frac{\beta_2}{2M^3} \nabla^2 Q (\nabla Q)^2 + \dots, \quad (1.4)$$

$$\mathcal{L}_{int}^{(4)} = -\frac{\tilde{\gamma}}{8M^4} (\nabla Q)^4 + \dots. \quad (1.5)$$

Here we only take the leading order interaction terms into account. We need to remind that the term of $\nabla^2 Q (\nabla Q)^2$ breaks the symmetry $Q \rightarrow -Q$ and $t \rightarrow -t$ which corresponds to $\phi \rightarrow -\phi$ for the ghost Lagrangian, and one may worry about the violation of CPT symmetry. However, the size of the CPT violating operator depends on the coupling of the ghost sector to ordinary matter and it is not predicted. The bispectrum from this term is expected to be similar to that from $\dot{Q} (\nabla Q)^2$ [16]. In this paper, we keep this term in the action and calculate the trispectrum related to this term as well.

Our results are not included in the previous discussions about the trispectrum in the general Lorentz invariant single-field inflation [18, 19, 20, 21, 22, 23, 24] and multi-field cases [25, 26, 27, 28], because the action for the quantum fluctuation Q breaks the Lorentz invariance. Our results are reliable at energies lower than the ghost cur-off M .

This paper is organized as follows. In Sec. 2 we repeat the calculation of the primordial power spectrum which is necessary for us to work out the non-Gaussianity parameters. In Sec. 3 we compute the trispectrum contributed from the contact and scalar-exchange diagram in ghost inflation. The conclusion and some discussions are contained in Sec. 4.

2. The Hamiltonian density in the interaction picture

From (1.3), the conjugate field Π in Heisenberg picture is defined as

$$\Pi = \frac{\partial \mathcal{L}}{\partial \dot{Q}} = \dot{Q} - \frac{\beta_1}{2M^2}(\nabla Q)^2, \quad (2.1)$$

and then \dot{Q} is related to the conjugate field by

$$\dot{Q} = \Pi + \frac{\beta_1}{2M^2}(\nabla Q)^2. \quad (2.2)$$

The Hamiltonian density becomes

$$\begin{aligned} \mathcal{H} &= \dot{Q}\Pi - \mathcal{L} \\ &= \frac{1}{2}\Pi^2 + \frac{\alpha^2}{2M^2}(\nabla^2 Q)^2 + \frac{\beta_1}{2M^2}\Pi(\nabla Q)^2 + \frac{\beta_2}{2M^3}\nabla^2 Q(\nabla Q)^2 + \frac{\gamma}{8M^4}(\nabla Q)^4, \end{aligned} \quad (2.3)$$

where

$$\gamma = \tilde{\gamma} + \beta_1^2. \quad (2.4)$$

In order to calculate four-point correlation function, we switch to the interaction representation and quantize this field theory. The fields Q and Π should be replaced by Q_I and Π_I in the interaction picture. Here the subscript ‘ I ’ denotes that the operators are in the interaction representation. The free-particle Hamiltonian density is adopted as

$$\mathcal{H}_0 = \frac{1}{2}\Pi_I^2 + \frac{\alpha^2}{2M^2}(\nabla Q_I)^2, \quad (2.5)$$

and the commutation relation between operators Q_I and Π_I is given by

$$[Q_I, \Pi_I] = i. \quad (2.6)$$

The time derivative of Q_I is

$$\dot{Q}_I = -i[Q_I, \mathcal{H}_0] = \frac{\partial \mathcal{H}_0}{\partial \Pi_I} = \Pi_I. \quad (2.7)$$

Therefore the interaction Hamiltonian density becomes

$$\mathcal{H}_I = \mathcal{H} - \mathcal{H}_0 = \frac{\beta_1}{2M^2}\dot{Q}_I(\nabla Q_I)^2 + \frac{\beta_2}{2M^3}\nabla^2 Q_I(\nabla Q_I)^2 + \frac{\gamma}{8M^4}(\nabla Q_I)^4. \quad (2.8)$$

From now on we omit the subscript ‘ I ’ in the variables. ¹

¹Our result is different from that in [36] where $\gamma = \tilde{\gamma} + 2\beta_1^2$.

3. The power spectrum

In [17], the authors showed that the gravitational potential Φ decays to zero outside the horizon. It implies that the fluctuations of Q do not gravitate at the superhorizon scales in the pure de Sitter space. Here we focus on the gauge invariant quantity which is related to Q by

$$\zeta = -\frac{H}{\dot{\phi}}Q = -\frac{H}{M^2}Q. \quad (3.1)$$

This quantity is conserved outside the horizon and it will seed the temperature fluctuations in the cosmic microwave background radiation.

In presence of ghost condensate gravity is modified in the IR region. This modification is characterized by a typical time scale Γ^{-1} with $\Gamma \sim M^3/M_p^2$, and a typical length scale m^{-1} with $m \sim M^2/M_p$ [17]. Requiring that gravity is not modified nowadays on the scales smaller than the present Hubble horizon, we need to impose $\Gamma < H_0$, where H_0 is present Hubble parameter. Therefore we have $\Gamma \ll m \ll H$, and the gravity is not modified during inflation.

From the action (1.3), at the linear level, we have

$$\ddot{Q} + 3H\dot{Q} + \frac{\alpha^2}{M^2}\nabla^4 Q = 0, \quad (3.2)$$

where

$$\nabla^2 = g^{ij}\partial_i\partial_j = \frac{1}{a^2}\partial_i\partial_i. \quad (3.3)$$

The field Q is canonically quantized as

$$Q(\mathbf{x}, t) = \int \frac{d^3k}{(2\pi)^3} Q_{\mathbf{k}}(t) e^{i\mathbf{k}\cdot\mathbf{x}}, \quad (3.4)$$

with

$$Q_{\mathbf{k}}(t) = q_k(t)\hat{a}_{\mathbf{k}} + q_k^*(t)\hat{a}_{-\mathbf{k}}^+, \quad (3.5)$$

and

$$[\hat{a}_{\mathbf{k}}, \hat{a}_{-\mathbf{k}'}^+] = (2\pi)^3 \delta^{(3)}(\mathbf{k} + \mathbf{k}'). \quad (3.6)$$

Here \mathbf{k} is the comoving wavevector, and $q_k(t)$ is governed by

$$\ddot{q}_k + 3H\dot{q}_k + \frac{\alpha^2}{M^2} \frac{k^4}{a^4} q_k = 0. \quad (3.7)$$

We introduce a new time coordinate, so-called conformal time τ which is related to t by

$$d\tau = \frac{dt}{a(t)}. \quad (3.8)$$

For an inflationary universe, we have

$$a = -\frac{1}{H\tau}, \quad (3.9)$$

where H is the Hubble parameter which can be taken as a constant in ghost inflation. Now the equation for the variable

$$u_k = a(\tau) \cdot q_k \quad (3.10)$$

becomes

$$u_k'' + \left(\frac{\alpha^2 H^2 k^4}{M^2} \tau^2 - \frac{2}{\tau^2} \right) u_k = 0, \quad (3.11)$$

where the prime denotes the derivative with respect to the conformal time τ . The solution of the above differential equation with the correct flat space limit for the very short physical wave-length ($\tau \rightarrow -\infty$) is given by

$$u_k(\tau) = \sqrt{\frac{\pi}{8}} \sqrt{-\tau} H_{3/4}^{(1)} \left(\frac{\alpha H k^2}{2M} \tau^2 \right), \quad (3.12)$$

where $H_\nu^{(1)}$ is the Hankel function of the first kind. Considering $q_k = u_k/a(\tau) = -H\tau \cdot u_k$, we obtain

$$q_k(\tau) = \sqrt{\frac{\pi}{8}} H \cdot (-\tau)^{3/2} H_{3/4}^{(1)} \left(\frac{\alpha H k^2}{2M} \tau^2 \right). \quad (3.13)$$

The power spectrum can be calculated from the asymptotic behavior in the limit of $\tau \rightarrow 0$. In this limit, we find

$$q_k(\tau \rightarrow 0) \simeq -\frac{i\sqrt{2\pi}}{\Gamma(1/4)} H \left(\frac{M}{\alpha H} \right)^{3/4} k^{-3/2}. \quad (3.14)$$

From the definition of power spectrum $P_\zeta(k)$, namely

$$\langle \zeta_{\mathbf{k}} \zeta_{\mathbf{k}'} \rangle = (2\pi)^3 \delta^{(3)}(\mathbf{k} + \mathbf{k}') \frac{2\pi^2}{k^3} P_\zeta(k), \quad (3.15)$$

we can easily calculate the amplitude of the primordial curvature perturbation,

$$P_\zeta = \frac{1}{\pi \Gamma^2(1/4)} \left(\frac{H}{M} \right)^{5/2} \alpha^{-3/2}. \quad (3.16)$$

Our results is the same as that in [16]. Using the WMAP normalization $P_\zeta = 2.41 \times 10^{-9}$ [14], we obtain

$$\frac{H}{M} \simeq 1.58 \times 10^{-3} \alpha^{3/5}. \quad (3.17)$$

Since $\Gamma \sim M^3/M_p^2 \ll H_0$ which implies $M \lesssim 10^{-20} M_p$, the energy scale of inflation is so small compared to Planck scale that the gravitational wave perturbation in ghost inflation must be completely negligible.

4. The trispectrum

In this section, we will explicitly calculate the four-point correlation function of the curvature perturbation in ghost inflation and discuss the shape of trispectrum.

A well established non-Gaussianity has a local shape. For the local shape non-Gaussianity, the curvature perturbation ζ can be expanded to the non-linear orders at the same spatial point,

$$\zeta(\mathbf{x}) = \zeta_g(\mathbf{x}) + \frac{3}{5}f_{NL}^{loc}\zeta_g^2(\mathbf{x}) + \frac{9}{25}g_{NL}^{loc}\zeta_g^3(\mathbf{x}) + \dots, \quad (4.1)$$

where ζ_g is the Gaussian part of curvature perturbation. The four-point irreducible correlation function of curvature perturbations are related to the power spectrum by

$$\langle \zeta_{\mathbf{k}_1} \zeta_{\mathbf{k}_2} \zeta_{\mathbf{k}_3} \zeta_{\mathbf{k}_4} \rangle = (2\pi)^9 \delta^{(3)}\left(\sum_{i=1}^4 \mathbf{k}_i\right) T_\zeta(k_1, k_2, k_3, k_4), \quad (4.2)$$

where

$$T_\zeta(k_1, k_2, k_3, k_4) = \frac{27}{100}g_{NL}^{loc}P_\zeta^3 \cdot \frac{\sum_{i=1}^4 k_i^3}{\prod_{i=1}^4 k_i^3} \quad (4.3)$$

$$+ \frac{1}{16}\tau_{NL}^{loc}P_\zeta^3 \cdot \left(\frac{1}{k_{12}^3 k_2^3 k_3^3} + 23 \text{ perms.} \right), \quad (4.4)$$

and $k_{12} = k_{34}$, $k_{13} = k_{24}$ etc. Here

$$\mathbf{k}_{ij} = \mathbf{k}_i + \mathbf{k}_j. \quad (4.5)$$

If $g_{NL}^{loc} \neq 0$, the term of g_{NL}^{loc} blows up when one or two of k_i goes to zero. If the curvature perturbation is generated by single scalar field, we get a consistency relation, namely $\tau_{NL}^{loc} = (\frac{6}{5}f_{NL}^{loc})^2$. If $\tau_{NL}^{loc} > (\frac{6}{5}f_{NL}^{loc})^2$, the curvature perturbation must be generated by more than one scalar fields. From (4.4), the term with τ_{NL}^{loc} also blows up when one or two of k_i goes to zero. The distinguishing feature for the term of τ_{NL}^{loc} is that the local form trispectrum blows up in the limit of $k_{ij} \rightarrow 0$, even when $k_1 = k_2 = k_3 = k_4 \neq 0$. Because the local shape trispectrum does blow up for these special configurations in the momenta space, it is much more sensitive to the cosmological observations than that with non-local shape.

The energy-momentum conservation implies that the four momenta vectors \mathbf{k}_i ($i = 1, 2, 3, 4$) form a quadrangle which is much more complicated than the triangle for the bispectrum. Its shape cannot be fixed even when the sizes of these four vectors are fixed. In this paper, we suggest a few special configurations.

- Planar mirror symmetric quadrangle. See Fig. 1. Here $\theta_1 \in [0, \pi]$ and $\theta_2 \in [0, \pi/2]$,

$$k_1 = k_2 = k, \quad k_3 = k_4 = \frac{\sin \frac{\theta_1}{2}}{\cos \theta_2} k \quad (4.6)$$

and

$$\frac{\mathbf{k}_1 \cdot \mathbf{k}_2}{k^2} = -\cos \theta_1, \quad \frac{\mathbf{k}_3 \cdot \mathbf{k}_4}{k^2} = \left(\frac{\sin \frac{\theta_1}{2}}{\cos \theta_2} \right)^2 \cos(2\theta_2), \quad (4.7)$$

$$\frac{\mathbf{k}_1 \cdot \mathbf{k}_3}{k^2} = \frac{\mathbf{k}_2 \cdot \mathbf{k}_4}{k^2} = -\frac{\sin \frac{\theta_1}{2}}{\cos \theta_2} \sin\left(\frac{\theta_1}{2} + \theta_2\right), \quad (4.8)$$

$$\frac{\mathbf{k}_1 \cdot \mathbf{k}_4}{k^2} = \frac{\mathbf{k}_2 \cdot \mathbf{k}_3}{k^2} = -\frac{\sin \frac{\theta_1}{2}}{\cos \theta_2} \sin\left(\frac{\theta_1}{2} - \theta_2\right). \quad (4.9)$$

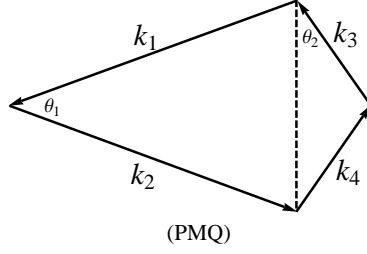


Figure 1: The planar mirror symmetric quadrangle shape.

If $\theta_2 = \pi/3$, in the limit of $\theta_1 \rightarrow 0$, $k_3 = k_4 = k_{12} = k_{34} \simeq \theta_1 k$ and the local form trispectrum becomes

$$T_\zeta(k_1, k_2, k_3, k_4) \simeq \frac{1}{2} \left(\frac{27}{25} g_{NL}^{loc.} + \tau_{NL}^{loc.} \right) \frac{P_\zeta^3}{\theta_1^6 k^9} \quad (4.10)$$

which goes to infinity. If $\theta_2 = (\pi - \theta_1)/2$, $k_1 = k_2 = k_3 = k_4$. In this case $k_{12} = k_{34} \simeq \theta_1 k$ in the limit of $\theta_1 \rightarrow 0$, and hence

$$T_\zeta(k_1, k_2, k_3, k_4) \simeq \frac{1}{2} \tau_{NL}^{loc.} \frac{P_\zeta^3}{\theta_1^3 k^9} \quad (4.11)$$

which also blows up for non-vanishing $\tau_{NL}^{loc.}$.

• Equilateral shape. Now $k_1 = k_2 = k_3 = k_4 \equiv k$, but there are still two extra degrees of freedom: the angle θ_{12} between the vector \mathbf{k}_1 and \mathbf{k}_2 , and the angle θ_{14} between the vector \mathbf{k}_1 and \mathbf{k}_4 . The angle between \mathbf{k}_1 and \mathbf{k}_3 is not an independent parameter which is related to θ_{12} and θ_{14} by

$$\theta_{13} = \pi - \cos^{-1}(1 + \cos \theta_{12} + \cos \theta_{14}). \quad (4.12)$$

In this case we have

$$\frac{\mathbf{k}_1 \cdot \mathbf{k}_2}{k^2} = \frac{\mathbf{k}_3 \cdot \mathbf{k}_4}{k^2} = \cos \theta_{12}, \quad (4.13)$$

$$\frac{\mathbf{k}_1 \cdot \mathbf{k}_3}{k^2} = \frac{\mathbf{k}_2 \cdot \mathbf{k}_4}{k^2} = \cos \theta_{13}, \quad (4.14)$$

$$\frac{\mathbf{k}_1 \cdot \mathbf{k}_4}{k^2} = \frac{\mathbf{k}_2 \cdot \mathbf{k}_3}{k^2} = \cos \theta_{14}. \quad (4.15)$$

The consistency condition for formation of a quadrangle is given by

$$\cos \theta_{12} + \cos \theta_{14} \leq 0. \quad (4.16)$$

Because all of the momenta vectors are finite, the term of $g_{NL}^{loc.}$ in the local form trispectrum is still finite, but the term of $\tau_{NL}^{loc.}$ can go to infinity when one or two of θ_{1i} ($i = 2, 3, 4$) goes to π . For example, if $\theta_{12} \rightarrow \pi$, we find

$$T_\zeta(k_1, k_2, k_3, k_4) \simeq \frac{1}{2} \tau_{NL}^{loc.} \frac{P_\zeta^3}{(\pi - \theta_{12})^3 k^9}. \quad (4.17)$$

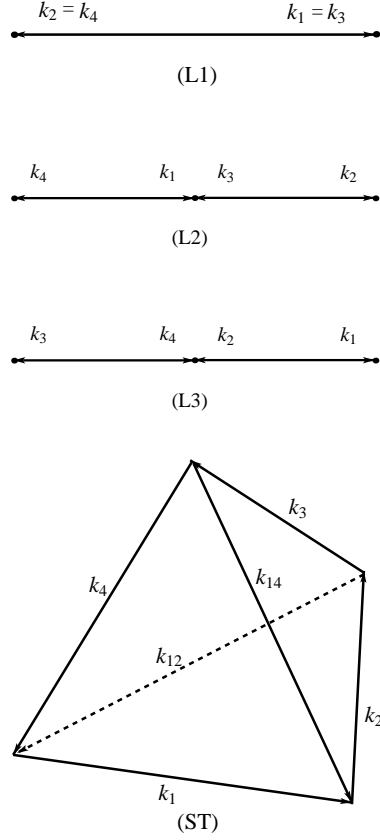


Figure 2: The special configurations in the momenta space for the trispectrum.

Here we suggest several special equilateral configurations, named L1, L2, L3, and ST (special tetrahedron) in Fig. 2. The angles θ_{12} and θ_{14} take the values for these configurations as follows

$$\text{L1 : } \quad \theta_{12} = \theta_{14} = \pi, \quad (4.18)$$

$$\text{L2 : } \quad \theta_{12} = 0, \quad \theta_{14} = \pi, \quad (4.19)$$

$$\text{L3 : } \quad \theta_{12} = \pi, \quad \theta_{14} = 0, \quad (4.20)$$

$$\text{ST : } \quad \theta_{12} = \theta_{14} = \cos^{-1}(-1/3). \quad (4.21)$$

For the shape “ST”, $k_{12} = k_{14} = k_{13} = 2k/\sqrt{3}$.

At the leading order, not only $\mathcal{H}_{int}^{(4)}$ but also $\mathcal{H}_{int}^{(3)}$ contribute to the trispectrum in ghost inflation. We will calculate the trispectrum generated by these two interaction terms in the following two subsections respectively.

4.1 Contact diagram

In this subsection, we compute the four-point correlation function from the contact interaction diagram illustrated in Fig. 3. This diagram corresponds to the interaction term

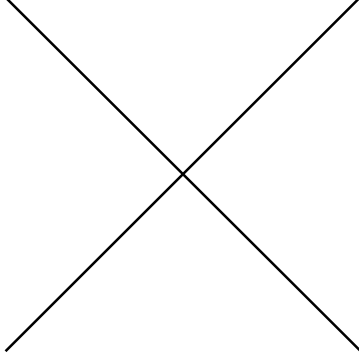


Figure 3: The contact interaction.

$\mathcal{L}_{int}^{(4)}$. In this case, $\langle Q_{\mathbf{k}_1} Q_{\mathbf{k}_2} Q_{\mathbf{k}_3} Q_{\mathbf{k}_4} \rangle$ is given by

$$\langle Q_{\mathbf{k}_1}(t) Q_{\mathbf{k}_2}(t) Q_{\mathbf{k}_3}(t) Q_{\mathbf{k}_4}(t) \rangle \supset -i \int_{t_0}^t dt' \left\langle \left[Q_{\mathbf{k}_1}(t) Q_{\mathbf{k}_2}(t) Q_{\mathbf{k}_3}(t) Q_{\mathbf{k}_4}(t), H_I^{(4)}(t') \right] \right\rangle, \quad (4.22)$$

where

$$H_I^{(4)} = \int d^3x \mathcal{H}_{int}^{(4)}, \quad (4.23)$$

and

$$\mathcal{H}_{int}^{(4)} = \frac{\gamma}{8M^4} \frac{1}{a(t)} (\partial_i Q \cdot \partial_i Q)^2. \quad (4.24)$$

Considering

$$\zeta_{\mathbf{k}} = -\frac{H}{M^2} Q_{\mathbf{k}}, \quad (4.25)$$

we obtain

$$\begin{aligned} \langle \zeta_{\mathbf{k}_1} \zeta_{\mathbf{k}_2} \zeta_{\mathbf{k}_3} \zeta_{\mathbf{k}_4} \rangle &\supset -i(2\pi)^3 \delta^{(3)} \left(\sum_{i=1}^4 \mathbf{k}_i \right) \cdot \gamma \cdot \frac{H^4}{M^{12}} \cdot \prod_{i=1}^4 q_{k_i}(0) \\ &\times \int_{-\infty}^0 d\tau \cdot \prod_i q_{k_i}^*(\tau) \cdot (\mathbf{k}_1 \cdot \mathbf{k}_2)(\mathbf{k}_3 \cdot \mathbf{k}_4) \\ &+ \text{symm.} + c.c. \end{aligned} \quad (4.26)$$

which is evaluated as

$$\begin{aligned} \langle \zeta_{\mathbf{k}_1} \zeta_{\mathbf{k}_2} \zeta_{\mathbf{k}_3} \zeta_{\mathbf{k}_4} \rangle &\supset +i(2\pi)^9 \delta^{(3)} \left(\sum_{i=1}^4 \mathbf{k}_i \right) \frac{\gamma}{2^{10} \cdot \pi^2 \cdot \Gamma^4(1/4)} \left(\frac{H}{M} \right)^{\frac{11}{2}} \alpha^{-\frac{13}{2}} \frac{(\mathbf{k}_1 \cdot \mathbf{k}_2)(\mathbf{k}_3 \cdot \mathbf{k}_4)}{k^7 \prod_i k_i^{3/2}} \\ &\times \int_{-\infty}^0 dx \cdot x^6 \cdot H_{3/4}^{(1)} \left(\frac{k_1^2 x^2}{k^2} \frac{x^2}{2} \right) H_{3/4}^{(1)} \left(\frac{k_2^2 x^2}{k^2} \frac{x^2}{2} \right) H_{3/4}^{(1)} \left(\frac{k_3^2 x^2}{k^2} \frac{x^2}{2} \right) H_{3/4}^{(1)} \left(\frac{k_4^2 x^2}{k^2} \frac{x^2}{2} \right) \\ &+ \text{symm.} + c.c. , \end{aligned} \quad (4.27)$$

where

$$x = \left(\frac{\alpha H}{M} \right)^{\frac{1}{2}} k \tau. \quad (4.28)$$

This is the full trispectrum from the contact interaction diagram. It is very difficult to get the analytic result. We will evaluate the numerical results for the special shapes in our previous discussions. Comparing to the local form trispectrum, we effectively define the non-Gaussianity parameters g_{NL} as follows

$$T_\zeta(k_1, k_2, k_3, k_4) \supset \frac{27}{100} g_{NL} P_\zeta^3 \cdot \frac{\sum_{i=1}^4 k_i^3}{\prod_{i=1}^4 k_i^3}. \quad (4.29)$$

In general g_{NL} is not a constant, but a function which depends on k_i . For the non-local shape trispectrum, g_{NL} goes to zero in the limit where one or two of k_i go to zero.

For the planar mirror symmetric quadrangle shape in Fig. 1, the “effective” non-Gaussianity parameter g_{NL}^{pmq} depends on the angles θ_1 and θ_2 ,

$$g_{NL}^{pmq} = -0.149 \cdot \gamma \cdot \frac{M^2}{H^2} \alpha^{-2} \cdot F_1(\theta_1, \theta_2), \quad (4.30)$$

where $F_1(\theta_1, \theta_2)$ shows up in Fig. 4. Combing with the WMAP normalization (3.17), we

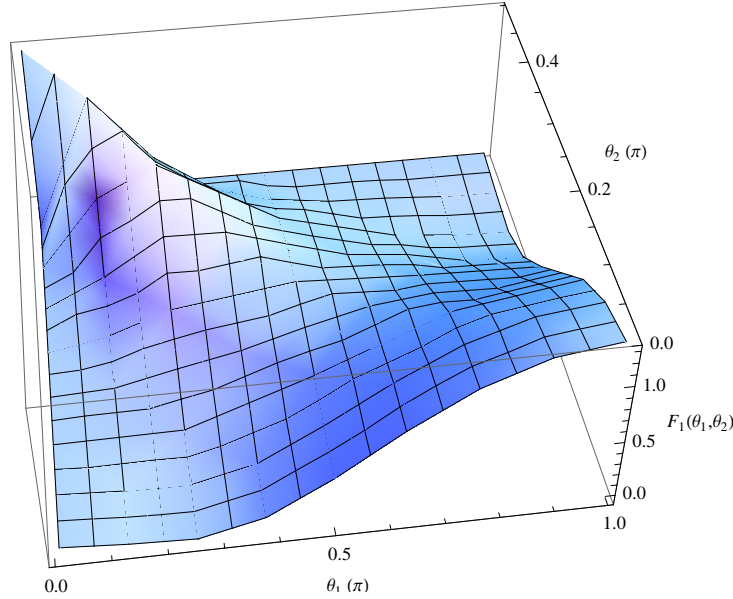


Figure 4: The function $F_1(\theta_1, \theta_2)$.

obtain

$$g_{NL}^{pmq} = -6 \times 10^4 \cdot \gamma \cdot \alpha^{-16/5} \cdot F_1(\theta_1, \theta_2). \quad (4.31)$$

For $\theta_2 = \pi/3$, $g_{NL}^{pmq} \rightarrow 0$ in the limit of $\theta_1 \rightarrow 0$. The local form trispectrum cannot be generated by the contact diagram in ghost inflation.

Similarly, the “effective” $g_{NL}^{equil.}$ for the equilateral shape is given by

$$g_{NL}^{equil.} \simeq -0.066 \cdot \gamma \cdot \frac{M^2}{H^2} \alpha^{-2} \cdot F_2(\theta_{12}, \theta_{14}), \quad (4.32)$$

where

$$F_2(\theta_{12}, \theta_{14}) = \cos^2 \theta_{12} + \cos^2 \theta_{14} + (1 + \cos \theta_{12} + \cos \theta_{14})^2. \quad (4.33)$$

The angle-dependent function $F(\theta_{12}, \theta_{14})$ is illustrated in Fig. 5. Combing with the WMAP

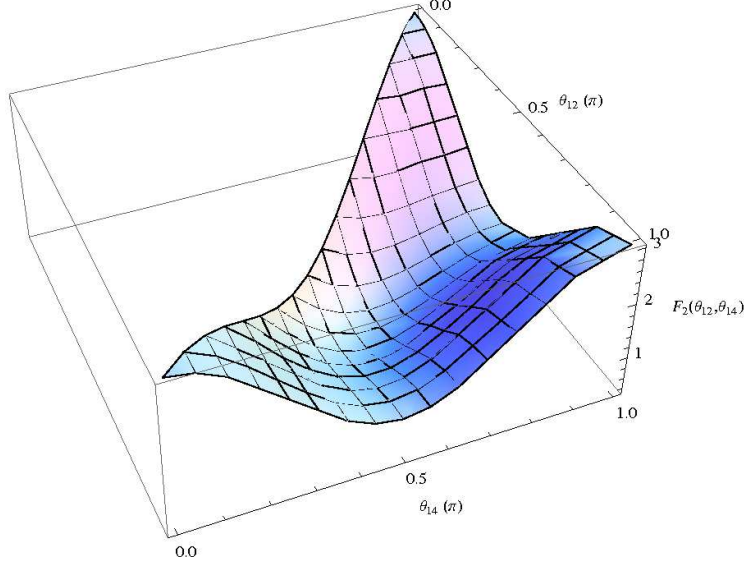


Figure 5: The function of $F_2(\theta_{12}, \theta_{14})$.

normalization (3.17), we obtain

$$g_{NL}^{equil.} \simeq -2.6 \times 10^4 \cdot \gamma \cdot \alpha^{-16/5} \cdot F_2(\theta_{12}, \theta_{14}), \quad (4.34)$$

For the special shapes in Fig. 2, we have

$$F_2^{L1} = F_2^{L2} = F_2^{L3} = 3, \quad (4.35)$$

$$F_2^{ST} = 1/3. \quad (4.36)$$

We see that the size of equilateral shape trispectrum from the contact interaction is maximized when these four equilateral momenta vectors lie in a straight line and minimized at the “ST” shape.

4.2 Scalar-exchange diagram

In this subsection, we switch to a more complicated case: the scalar-exchange diagram in Fig. 6. There are two vertices in this diagram. Each of them can come from the term characterized by β_1 or β_2 in $\mathcal{L}_{int}^{(3)}$. The four-point correlation function in the scalar-exchange

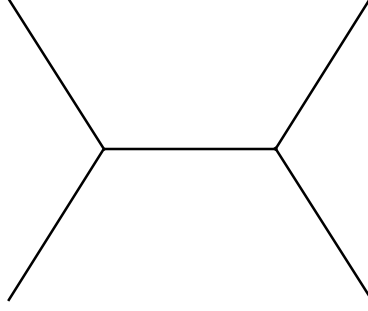


Figure 6: The scalar-exchange diagram.

diagram is given by, [29],

$$\langle Q_{\mathbf{k}_1} Q_{\mathbf{k}_2} Q_{\mathbf{k}_3} Q_{\mathbf{k}_4} \rangle \supset \int_{t_0}^t dt_1 \int_{t_0}^t dt_2 \langle 0 | H_I^{(3)}(t_1) Q_{\mathbf{k}_1} Q_{\mathbf{k}_2} Q_{\mathbf{k}_3} Q_{\mathbf{k}_4} H_I^{(3)}(t_2) | 0 \rangle \quad (4.37)$$

$$- 2\text{Re} \int_{t_0}^t dt_1 \int_{t_0}^{t_1} dt_2 \langle 0 | H_I^{(3)}(t_2) H_I^{(3)}(t_1) Q_{\mathbf{k}_1} Q_{\mathbf{k}_2} Q_{\mathbf{k}_3} Q_{\mathbf{k}_4} | 0 \rangle, \quad (4.38)$$

where

$$H_I^{(3)} = \int d^3x \mathcal{H}_{int}^{(3)}, \quad (4.39)$$

and

$$\mathcal{H}_{int}^{(3)} = -\mathcal{L}_{int}^{(3)} = \frac{\beta_1}{2M^2} \frac{d}{d\tau} Q \cdot \partial_i Q \cdot \partial_i Q + \frac{\beta_2}{2M^3} \frac{1}{a(t)} \partial_i \partial_i Q \cdot \partial_j Q \cdot \partial_j Q. \quad (4.40)$$

For simplicity, we assume that both of the vertices are contributed by the interaction term with β_1 firstly. We write down the results of Eq.(4.37) and (4.38) separately. Eq.(4.37) is

$$\begin{aligned} & (2\pi)^3 \delta^{(3)} \left(\sum_{i=1}^4 \mathbf{k}_i \right) \cdot \frac{\beta_1^2}{4M^4 H^2} \cdot q_{k_1}^*(0) q_{k_2}^*(0) q_{k_3}(0) q_{k_4}(0) \times \\ & \left\{ \int_{-\infty}^0 \frac{d\tau_1}{\tau_1} \frac{d}{d\tau_1} q_{k_{12}}(\tau_1) \cdot q_{k_1}(\tau_1) q_{k_2}(\tau_1) \right. \\ & \times \left[(\mathbf{k}_1 \cdot \mathbf{k}_2)(\mathbf{k}_3 \cdot \mathbf{k}_4) \int_{-\infty}^0 \frac{d\tau_2}{\tau_2} \cdot \frac{d}{d\tau_2} q_{k_{12}}^*(\tau_2) \cdot q_{k_3}^*(\tau_2) q_{k_4}^*(\tau_2) \right. \\ & + 2(\mathbf{k}_1 \cdot \mathbf{k}_2)(\mathbf{k}_{12} \cdot \mathbf{k}_4) \int_{-\infty}^0 \frac{d\tau_2}{\tau_2} \cdot q_{k_{12}}^*(\tau_2) \cdot \frac{d}{d\tau_2} q_{k_3}^*(\tau_2) \cdot q_{k_4}^*(\tau_2) \Big] \\ & + \int_{-\infty}^0 \frac{d\tau_1}{\tau_1} \cdot q_{k_{12}}(\tau_1) \cdot \frac{d}{d\tau_1} q_{k_1}(\tau_1) \cdot q_{k_2}(\tau_1) \\ & \times \left[-2(\mathbf{k}_{12} \cdot \mathbf{k}_2)(\mathbf{k}_3 \cdot \mathbf{k}_4) \int_{-\infty}^0 \frac{d\tau_2}{\tau_2} \cdot \frac{d}{d\tau_2} q_{k_{12}}^*(\tau_2) \cdot q_{k_3}^*(\tau_2) q_{k_4}^*(\tau_2) \right. \\ & \left. - 4(\mathbf{k}_{12} \cdot \mathbf{k}_2)(\mathbf{k}_{12} \cdot \mathbf{k}_4) \int_{-\infty}^0 \frac{d\tau_2}{\tau_2} \cdot q_{k_{12}}^*(\tau_2) \cdot \frac{d}{d\tau_2} q_{k_3}^*(\tau_2) \cdot q_{k_4}^*(\tau_2) \right] \Big\} \\ & + 23 \text{ perms.} \end{aligned} \quad (4.41)$$

Eq.(4.38) is

$$\begin{aligned}
& -2(2\pi)^3 \delta^{(3)} \left(\sum_{i=1}^4 \mathbf{k}_i \right) \cdot \frac{\beta_1^2}{4M^4 H^2} \cdot q_{k_1}^*(0) q_{k_2}^*(0) q_{k_3}^*(0) q_{k_4}^*(0) \times \\
& \text{Re} \left\{ \int_{-\infty}^0 \frac{d\tau_1}{\tau_1} \frac{d}{d\tau_1} q_{k_{12}}^*(\tau_1) \cdot q_{k_3}(\tau_1) q_{k_4}(\tau_1) \right. \\
& \times \left[(\mathbf{k}_1 \cdot \mathbf{k}_2)(\mathbf{k}_3 \cdot \mathbf{k}_4) \int_{-\infty}^{\tau_1} \frac{d\tau_2}{\tau_2} \cdot \frac{d}{d\tau_2} q_{k_{12}}(\tau_2) \cdot q_{k_1}(\tau_2) q_{k_2}(\tau_2) \right. \\
& \left. - 2(\mathbf{k}_{12} \cdot \mathbf{k}_2)(\mathbf{k}_3 \cdot \mathbf{k}_4) \int_{-\infty}^{\tau_1} \frac{d\tau_2}{\tau_2} \cdot q_{k_{12}}(\tau_2) \cdot \frac{d}{d\tau_2} q_{k_1}(\tau_2) \cdot q_{k_2}(\tau_2) \right] \\
& + \int_{-\infty}^0 \frac{d\tau_1}{\tau_1} \cdot q_{k_{12}}^*(\tau_1) \cdot \frac{d}{d\tau_1} q_{k_3}(\tau_1) \cdot q_{k_4}(\tau_1) \\
& \times \left[2(\mathbf{k}_1 \cdot \mathbf{k}_2)(\mathbf{k}_{12} \cdot \mathbf{k}_4) \int_{-\infty}^{\tau_1} \frac{d\tau_2}{\tau_2} \cdot \frac{d}{d\tau_2} q_{k_{12}}(\tau_2) \cdot q_{k_1}(\tau_2) q_{k_2}(\tau_2) \right. \\
& \left. - 4(\mathbf{k}_{12} \cdot \mathbf{k}_2)(\mathbf{k}_{12} \cdot \mathbf{k}_4) \int_{-\infty}^{\tau_1} \frac{d\tau_2}{\tau_2} \cdot q_{k_{12}}(\tau_2) \cdot \frac{d}{d\tau_2} q_{k_1}(\tau_2) \cdot q_{k_2}(\tau_2) \right] \Big\} \\
& + 23 \text{ perms.} \tag{4.42}
\end{aligned}$$

We can do the similar calculations for the term with β_2 and the cross case.

For the scalar-exchange diagram, $T_\zeta(k_1, k_2, k_3, k_4)$ also depends on k_{ij} . However, in general, we cannot effectively define the non-Gaussianity parameter τ_{NL} because the coefficients for different $\frac{1}{k_{ij}^3 k_j^3 k_l^3}$ might be different for a given momenta configuration. Based on the symmetry of the four-point correlation function, we define three new parameters $\tau^{(i)}$ with $i = 1, 2, 3$ for the general equilateral shape trispectrum ($k_1 = k_2 = k_3 = k_4 \equiv k$),

$$\langle \zeta_{\mathbf{k}_1} \zeta_{\mathbf{k}_2} \zeta_{\mathbf{k}_3} \zeta_{\mathbf{k}_4} \rangle \supset (2\pi)^9 \delta^{(3)} \left(\sum_{i=1}^4 \mathbf{k}_i \right) \cdot \frac{1}{16} P_\zeta^3 \times \Xi(k_i, k_{ij}), \tag{4.43}$$

where

$$\begin{aligned}
\Xi(k_i, k_{ij}) = & \tau^{(1)} \left(\frac{1}{k_{12}^3 k_2^3 k_3^3} + \frac{1}{k_{12}^3 k_2^3 k_4^3} + \frac{1}{k_{21}^3 k_1^3 k_3^3} + \frac{1}{k_{21}^3 k_1^3 k_4^3} + (1 \leftrightarrow 3, 2 \leftrightarrow 4) \right) \\
& + \tau^{(2)} \left(\frac{1}{k_{13}^3 k_3^3 k_2^3} + \frac{1}{k_{13}^3 k_3^3 k_4^3} + \frac{1}{k_{31}^3 k_1^3 k_2^3} + \frac{1}{k_{31}^3 k_1^3 k_4^3} + (1 \leftrightarrow 2, 3 \leftrightarrow 4) \right) \\
& + \tau^{(3)} \left(\frac{1}{k_{14}^3 k_4^3 k_2^3} + \frac{1}{k_{14}^3 k_4^3 k_3^3} + \frac{1}{k_{41}^3 k_1^3 k_2^3} + \frac{1}{k_{41}^3 k_1^3 k_3^3} + (1 \leftrightarrow 2, 3 \leftrightarrow 4) \right).
\end{aligned}$$

For the special equilateral shape “ST” in which $\theta_{12} = \theta_{13} = \theta_{14} = \cos^{-1}(-1/3)$, $k_{12} = k_{13} = k_{14} = \frac{2}{\sqrt{3}}k$, $\tau^{(1)} = \tau^{(2)} = \tau^{(3)}$ and then we can effectively define τ_{NL}^{ST} as follows

$$\langle \zeta_{\mathbf{k}_1} \zeta_{\mathbf{k}_2} \zeta_{\mathbf{k}_3} \zeta_{\mathbf{k}_4} \rangle \supset (2\pi)^9 \delta^{(3)} \left(\sum_{i=1}^4 \mathbf{k}_i \right) \cdot \frac{1}{16} \tau_{NL}^{ST} P_\zeta^3 \cdot \left(\frac{1}{k_{12}^3 k_2^3 k_3^3} + 23 \text{ perms.} \right), \tag{4.44}$$

where $\tau_{NL}^{ST} \equiv \tau^{(1)} = \tau^{(2)} = \tau^{(3)}$ at “ST” shape.

Considering $\zeta_{\mathbf{k}} = -\frac{H}{M^2}Q_{\mathbf{k}}$, and

$$\frac{d}{d\tau}q_k(\tau) = -\sqrt{\frac{\pi}{8}}\frac{\alpha H^2}{M}k^2(-\tau)^{5/2}H_{-1/4}^{(1)}\left(\frac{\alpha H k^2}{2M}\tau^2\right), \quad (4.45)$$

we find

$$\begin{aligned} \tau^{(i)} \simeq & 0.0437 \cdot \beta_1^2 \cdot \frac{M^2}{H^2} \cdot \alpha^{-2} \cdot T_{\beta_1, \beta_1}(\Theta_i) + 0.492 \cdot \beta_2^2 \cdot \frac{M^2}{H^2} \cdot \alpha^{-4} \cdot T_{\beta_2, \beta_2}(\Theta_i) \\ & - 0.156 \cdot \beta_1 \beta_2 \cdot \frac{M^2}{H^2} \cdot \alpha^{-3} \cdot T_{\beta_1, \beta_2}(\Theta_i), \end{aligned} \quad (4.46)$$

where $i = 1, 2, 3$, and $\Theta_1 = \theta_{12}$, $\Theta_2 = \theta_{13}$, $\Theta_3 = \theta_{14}$. Combining with WMAP normalization, we obtain

$$\begin{aligned} \tau^{(i)} \simeq & 1.75 \times 10^4 \cdot \beta_1^2 \cdot \alpha^{-16/5} \cdot T_{\beta_1, \beta_1}(\Theta_i) + 1.97 \times 10^5 \cdot \beta_2^2 \cdot \alpha^{-26/5} \cdot T_{\beta_2, \beta_2}(\Theta_i) \\ & - 6.25 \times 10^4 \cdot \beta_1 \beta_2 \cdot \alpha^{-21/5} \cdot T_{\beta_1, \beta_2}(\Theta_i), \end{aligned} \quad (4.47)$$

where $T_{\beta_1, \beta_1}(\Theta)$, $T_{\beta_1, \beta_2}(\Theta)$ and $T_{\beta_2, \beta_2}(\Theta)$ are showed in Fig. 7. Here we normalized these

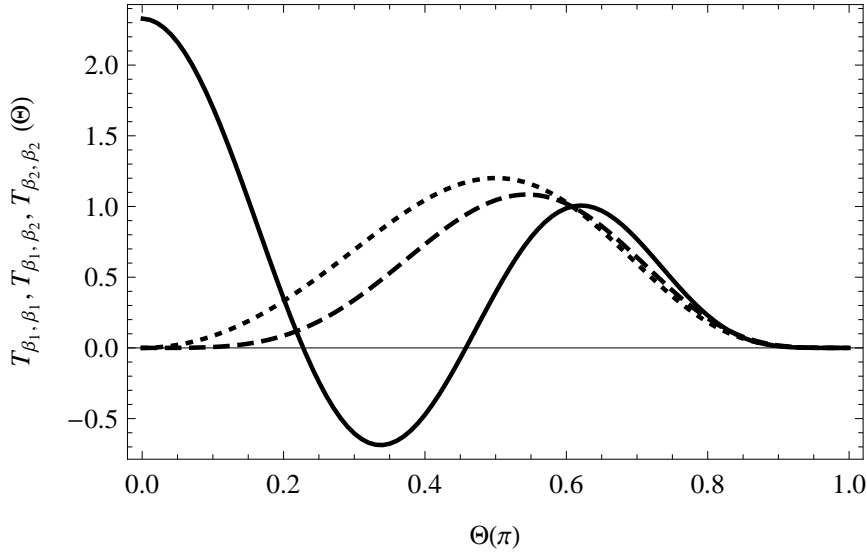


Figure 7: The functions $T_{\beta_1, \beta_1}(\Theta)$, $T_{\beta_1, \beta_2}(\Theta)$ and $T_{\beta_2, \beta_2}(\Theta)$ which correspond to the solid, dotted and dashed lines.

three functions at $\Theta = \cos^{-1}(-1/3)$. From Fig. 7, we see that the contribution by $\dot{Q}(\nabla Q)^2$ is quite different from that by $\nabla^2 Q(\nabla Q)^2$. Roughly speaking, $\tau^{(i)}$ for $i = 1, 2, 3$ are peaked around the special tetrahedron shape where $\theta_{12} = \theta_{13} = \theta_{14} = \cos^{-1}(-1/3)$. For the local shape trispectrum, $T_\zeta(k_1, k_2, k_3, k_4)$ blows up for the shape of $k_{ij} \rightarrow 0$ which corresponds to $\theta_{ij} \rightarrow \pi$. But here $\tau^{(i)}$ goes to zero when $\theta_{ij} \rightarrow \pi$. Therefore the scalar-exchange diagram in the ghost inflation cannot generate a local shape trispectrum. For the “ST” shape, we

obtain

$$\begin{aligned}\tau_{NL}^{ST} &\simeq 1.75 \times 10^4 \cdot \beta_1^2 \cdot \alpha^{-16/5} + 1.97 \times 10^5 \cdot \beta_2^2 \cdot \alpha^{-26/5} \\ &\quad - 6.25 \times 10^4 \cdot \beta_1 \beta_2 \cdot \alpha^{-21/5}\end{aligned}\tag{4.48}$$

which is positive definite.

Actually there is not a distinguishing feature to define the analogous parameters to $g_{NL}^{loc.}$ and $\tau_{NL}^{loc.}$ for the non-local shape trispectrum. Since the trispectrum from the scalar-exchange diagram in ghost inflation does not blow up like that for the local shape trispectrum with non-zero $\tau_{NL}^{loc.}$ at the limit of $k_{ij} \rightarrow 0$, it is hard to make the meaning of τ_{NL}^{ST} clear. For example, we can also calculate the effective $g_{NL}^{equil.}$ defined in Eq. (4.29) for the trispectrum from scalar-exchange diagram. Comparing Eq. (4.43) with (4.29), we obtain

$$g_{NL}^{equil.} = \frac{25}{108} \Xi(k_i, k_{ij}) \times \frac{\prod_{i=1}^4 k_i^3}{\sum_{i=1}^4 k_i^3} = \frac{25}{432} k^9 \Xi(k_i, k_{ij}),\tag{4.49}$$

here we focus on the equilateral shape with $k_1 = k_2 = k_3 = k_4 \equiv k$. For the “ST” shape, $k_{12} = k_{13} = k_{14} = 2k/\sqrt{3}$ and then

$$\Xi^{ST} = \frac{9\sqrt{3}}{k^9} \tau_{NL}^{ST}.\tag{4.50}$$

Therefore

$$g_{NL}^{ST} = \frac{25\sqrt{3}}{48} \tau_{NL}^{ST},\tag{4.51}$$

where g_{NL}^{ST} is $g_{NL}^{equil.}$ evaluated at “ST” shape. Similarly, we can also define an effective τ_{NL}^{ST} for the contact diagram as

$$\tau_{NL}^{ST} = -9.61 \times 10^3 \cdot \gamma \cdot \alpha^{-16/5}.\tag{4.52}$$

Here γ denotes that it is contributed from the contact diagram.

For general equilateral shape, we have

$$\frac{k_{12}^2}{k^2} = 2(1 + \cos \theta_{12}),\tag{4.53}$$

$$\frac{k_{13}^2}{k^2} = 2(1 + \cos \theta_{13}),\tag{4.54}$$

$$\frac{k_{14}^2}{k^2} = 2(1 + \cos \theta_{14}),\tag{4.55}$$

and thus the effective non-gaussianity parameter contributed from the scalar-exchange diagram in ghost inflation is

$$\begin{aligned}g_{NL}^{equil.} &= \frac{25}{54} \left[\frac{\tau^{(1)}}{(2(1 + \cos \theta_{12}))^{3/2}} + \frac{\tau^{(2)}}{(2(1 + \cos \theta_{13}))^{3/2}} + \frac{\tau^{(3)}}{(2(1 + \cos \theta_{14}))^{3/2}} \right] \\ &\simeq 8.1 \times 10^3 \cdot \beta_1^2 \cdot \alpha^{-16/5} \cdot W_{\beta_1, \beta_1}(\theta_{12}, \theta_{14}) + 9.1 \times 10^4 \cdot \beta_2^2 \cdot \alpha^{-26/5} \cdot W_{\beta_2, \beta_2}(\theta_{12}, \theta_{14}) \\ &\quad - 2.9 \times 10^4 \cdot \beta_1 \beta_2 \cdot \alpha^{-21/5} \cdot W_{\beta_1, \beta_2}(\theta_{12}, \theta_{14}),\end{aligned}\tag{4.56}$$

where

$$\begin{aligned}
W_{\beta_1, \beta_1}(\theta_{12}, \theta_{14}) &= \frac{T_{\beta_1, \beta_1}(\theta_{12})}{(2(1 + \cos \theta_{12}))^{3/2}} + \frac{T_{\beta_1, \beta_1}(\theta_{13})}{(2(1 + \cos \theta_{13}))^{3/2}} + \frac{T_{\beta_1, \beta_1}(\theta_{14})}{(2(1 + \cos \theta_{14}))^{3/2}}, \\
W_{\beta_1, \beta_2}(\theta_{12}, \theta_{14}) &= \frac{T_{\beta_1, \beta_2}(\theta_{12})}{(2(1 + \cos \theta_{12}))^{3/2}} + \frac{T_{\beta_1, \beta_2}(\theta_{13})}{(2(1 + \cos \theta_{13}))^{3/2}} + \frac{T_{\beta_1, \beta_2}(\theta_{14})}{(2(1 + \cos \theta_{14}))^{3/2}}, \\
W_{\beta_2, \beta_2}(\theta_{12}, \theta_{14}) &= \frac{T_{\beta_2, \beta_2}(\theta_{12})}{(2(1 + \cos \theta_{12}))^{3/2}} + \frac{T_{\beta_2, \beta_2}(\theta_{13})}{(2(1 + \cos \theta_{13}))^{3/2}} + \frac{T_{\beta_2, \beta_2}(\theta_{14})}{(2(1 + \cos \theta_{14}))^{3/2}},
\end{aligned}$$

which are shown in Fig. 8 respectively. The parameter $g_{NL}^{equil.}$ is shape-dependent and $g_{NL}^{equil.}$ goes to zero when θ_{12} and/or θ_{14} go to π .

5. Discussions

In this paper we calculate the trispectrum from the contact and scalar-exchange diagram in ghost inflation. The shape of trispectrum generated by the contact diagram is quite different from that produced by the scalar-exchange diagram. Roughly speaking, the former is peaked at the shapes L1, L2, and L3 and minimized at the shape ST, but the later is the reverse.

In this paper, we introduce a new shape, so-called “planar mirror symmetric quadrangle” shape. This shape is very useful to distinguish the term with $\tau_{NL}^{loc.}$ in trispectrum from that with $g_{NL}^{loc.}$: in the case of $\theta_2 = (\pi - \theta_1)/2$ and $k_1 = k_2 = k_3 = k_4$, only the term with $\tau_{NL}^{loc.}$ blows up in the limit of $\theta_1 \rightarrow 0$; but both of them blow up in the limit of $\theta_1 \rightarrow 0$ when $\theta_2 = \pi/3$.

For the local form non-Gaussianity, the trispectrum is completely characterized by two independent parameters $\tau_{NL}^{loc.}$ and $g_{NL}^{loc.}$. However, for the general single-field inflation, including ghost inflation, the trispectrum does not blow up in the limit of $k_i \rightarrow 0$ and/or $k_{ij} \rightarrow 0$. For the non-local form trispectrum, the analogous to $\tau_{NL}^{loc.}$ can be defined only for the shape “ST”, but there is not a definite feature to distinguish τ_{NL}^{ST} from $g_{NL}^{equil.}$. In Sec. 4.2, we clearly illustrate that τ_{NL}^{ST} is nothing but g_{NL}^{ST} which is $g_{NL}^{equil.}$ evaluated at “ST” shape.

The trispectrum in the ghost inflation is quite different from that in the single-field inflation without breaking Lorentz symmetry. For example, DBI inflation, a typical inflation in string theory, predicts a definite positive value of τ_{NL}^{ST} , but it can be either positive or negative in ghost inflation. The trispectrum potentially provides a very useful discriminator for inflation models. However, how to define some observables which can be directly used to compare to the observational data is still an open question for the non-local shape trispectrum. Here we need to emphasize that the local form non-Gaussianity is much more sensitive to the cosmological observations [30, 31, 32, 33, 34, 35]. For example, the uncertainties of $f_{NL}^{loc.}$, $\tau_{NL}^{loc.}$ and $g_{NL}^{loc.}$ will be reduced to $\Delta f_{NL}^{loc.} = 5$, $\Delta \tau_{NL}^{loc.} \simeq 560$ and $\Delta g_{NL}^{loc.} \simeq 1.3 \times 10^4$ by Planck. A convincing detection of non-Gaussianity with local or non-local form will have a profound implication for the physics in the early universe.

Note added: After we submitted our paper to arXiv, a paper [36] working on the same topic appeared in arXiv as well. Actually our discussions are more complete. We considered contributions to the trispectrum from the terms of $\dot{Q}(\nabla Q)^2$ and $\nabla^2 Q(\nabla Q)^2$ and cross case in the scalar-exchange diagram. However in [36] the authors only took $\dot{Q}(\nabla Q)^2$ into account.

Acknowledgments

We would like to thank P. Chingangbam and P. Yi for useful discussions. This work is supported by the project of Knowledge Innovation Program of Chinese Academy of Science.

References

- [1] D. Babich, P. Creminelli and M. Zaldarriaga, “The shape of non-Gaussianities,” JCAP **0408**, 009 (2004) [arXiv:astro-ph/0405356].
- [2] D. H. Lyth, “Generating the curvature perturbation at the end of inflation,” JCAP **0511**, 006 (2005) [arXiv:astro-ph/0510443].
- [3] M. Sasaki, “Multi-brid inflation and non-Gaussianity,” Prog. Theor. Phys. **120**, 159 (2008) [arXiv:0805.0974 [astro-ph]].
- [4] Q. G. Huang, “The Trispectrum in the Multi-brid Inflation,” JCAP **0905**, 005 (2009) [arXiv:0903.1542 [hep-th]].
- [5] Q. G. Huang, “A geometric description of the non-Gaussianity generated at the end of multi-field inflation,” JCAP **0906**, 035 (2009) [arXiv:0904.2649 [hep-th]].
- [6] K. Enqvist and M. S. Sloth, “Adiabatic CMB perturbations in pre big bang string cosmology,” Nucl. Phys. B **626**, 395 (2002) [arXiv:hep-ph/0109214].
- [7] D. H. Lyth and D. Wands, “Generating the curvature perturbation without an inflaton,” Phys. Lett. B **524**, 5 (2002) [arXiv:hep-ph/0110002].
- [8] T. Moroi and T. Takahashi, “Effects of cosmological moduli fields on cosmic microwave background,” Phys. Lett. B **522**, 215 (2001) [Erratum-ibid. B **539**, 303 (2002)] [arXiv:hep-ph/0110096].
- [9] M. Sasaki, J. Valiviita and D. Wands, “Non-gaussianity of the primordial perturbation in the curvaton model,” Phys. Rev. D **74**, 103003 (2006) [arXiv:astro-ph/0607627].
- [10] Q. G. Huang, “Large Non-Gaussianity Implication for Curvaton Scenario,” Phys. Lett. B **669**, 260 (2008) [arXiv:0801.0467 [hep-th]].
- [11] Q. G. Huang, “The N-vaton,” JCAP **0809**, 017 (2008) [arXiv:0807.1567 [hep-th]].
- [12] Q. G. Huang, “A Curvaton with a Polynomial Potential,” JCAP **0811**, 005 (2008) [arXiv:0808.1793 [hep-th]].
- [13] C. T. Byrnes, M. Sasaki and D. Wands, “The primordial trispectrum from inflation,” Phys. Rev. D **74**, 123519 (2006) [arXiv:astro-ph/0611075];
T. Matsuda, “Modulated Inflation,” Phys. Lett. B **665**, 338 (2008) [arXiv:0801.2648 [hep-ph]];
Q. G. Huang, “Spectral Index in Curvaton Scenario,” Phys. Rev. D **78**, 043515 (2008) [arXiv:0807.0050 [hep-th]];
A. Naruko and M. Sasaki, “Large non-Gaussianity from multi-brid inflation,” Prog. Theor. Phys. **121**, 193 (2009) [arXiv:0807.0180 [astro-ph]];
C. T. Byrnes, K. Y. Choi and L. M. H. Hall, “Conditions for large non-Gaussianity in two-field slow-roll inflation,” JCAP **0810**, 008 (2008) [arXiv:0807.1101 [astro-ph]];
K. Enqvist and T. Takahashi, “Signatures of Non-Gaussianity in the Curvaton Model,” JCAP **0809**, 012 (2008) [arXiv:0807.3069 [astro-ph]];
Q. G. Huang and Y. Wang, “Curvaton Dynamics and the Non-Linearity Parameters in Curvaton Model,” JCAP **0809**, 025 (2008) [arXiv:0808.1168 [hep-th]];
M. Kawasaki, K. Nakayama and F. Takahashi, “Hilltop Non-Gaussianity,” JCAP **0901**, 026 (2009) [arXiv:0810.1585 [hep-ph]];
C. T. Byrnes, K. Y. Choi and L. M. H. Hall, “Large non-Gaussianity from two-component hybrid inflation,” JCAP **0902**, 017 (2009) [arXiv:0812.0807 [astro-ph]].

- P. Chingangbam and Q. G. Huang, “The Curvature Perturbation in the Axion-type Curvaton Model,” JCAP **0904**, 031 (2009) [arXiv:0902.2619 [astro-ph.CO]];
- T. Takahashi, M. Yamaguchi, J. Yokoyama and S. Yokoyama, “Gravitino Dark Matter and Non-Gaussianity,” Phys. Lett. B **678**, 15 (2009) [arXiv:0905.0240 [astro-ph.CO]];
- C. T. Byrnes and G. Tasinato, “Non-Gaussianity beyond slow roll in multi-field inflation,” arXiv:0906.0767 [astro-ph.CO];
- S. Renaux-Petel, “Combined local and equilateral non-Gaussianities from multifield DBI inflation,” arXiv:0907.2476 [hep-th];
- T. Takahashi, M. Yamaguchi and S. Yokoyama, “Primordial Non-Gaussianity in Models with Dark Matter Isocurvature Fluctuations,” arXiv:0907.3052 [astro-ph.CO];
- D. Battefeld and T. Battefeld, “On Non-Gaussianities in Multi-Field Inflation (N fields): Bi- and Tri-spectra beyond Slow-Roll,” arXiv:0908.4269 [hep-th];
- J. Kumar, L. Leblond and A. Rajaraman, “Scale Dependent Local Non-Gaussianity from Loops,” arXiv:0909.2040 [astro-ph.CO];
- K. Enqvist and T. Takahashi, “Effect of Background Evolution on the Curvaton Non-Gaussianity,” arXiv:0909.5362 [astro-ph.CO];
- K. Nakayama and J. Yokoyama, “Gravitational Wave Background and Non-Gaussianity as a Probe of the Curvaton Scenario,” arXiv:0910.0715 [astro-ph.CO];
- M. Kawasaki, T. Takahashi and S. Yokoyama, “Density Fluctuations in Thermal Inflation and Non-Gaussianity,” arXiv:0910.3053 [hep-th].
- [14] E. Komatsu *et al.*, “Seven-Year Wilkinson Microwave Anisotropy Probe (WMAP) Observations: Cosmological Interpretation,” arXiv:1001.4538 [astro-ph.CO].
- [15] Q. G. Huang, “Consistency relation for the Lorentz invariant single-field inflation,” JCAP **1005**, 016 (2010) [arXiv:1001.5110 [astro-ph.CO]].
- [16] N. Arkani-Hamed, P. Creminelli, S. Mukohyama and M. Zaldarriaga, “Ghost Inflation,” JCAP **0404**, 001 (2004) [arXiv:hep-th/0312100].
- [17] N. Arkani-Hamed, H. C. Cheng, M. A. Luty and S. Mukohyama, “Ghost condensation and a consistent infrared modification of gravity,” JHEP **0405**, 074 (2004) [arXiv:hep-th/0312099].
- [18] D. Seery, J. E. Lidsey and M. S. Sloth, “The inflationary trispectrum,” JCAP **0701**, 027 (2007) [arXiv:astro-ph/0610210].
- [19] D. Seery and J. E. Lidsey, “Non-gaussianity from the inflationary trispectrum,” JCAP **0701**, 008 (2007) [arXiv:astro-ph/0611034].
- [20] F. Arroja and K. Koyama, “Non-gaussianity from the trispectrum in general single field inflation,” Phys. Rev. D **77**, 083517 (2008) [arXiv:0802.1167 [hep-th]].
- [21] D. Seery, M. S. Sloth and F. Vernizzi, “Inflationary trispectrum from graviton exchange,” JCAP **0903**, 018 (2009) [arXiv:0811.3934 [astro-ph]].
- [22] X. Chen, B. Hu, M. x. Huang, G. Shiu and Y. Wang, “Large Primordial Trispectra in General Single Field Inflation,” arXiv:0905.3494 [astro-ph.CO].
- [23] F. Arroja, S. Mizuno, K. Koyama and T. Tanaka, “On the full trispectrum in single field DBI-inflation,” arXiv:0905.3641 [hep-th].
- [24] H. R. S. Cogollo, Y. Rodriguez and C. A. Valenzuela-Toledo, “On the Issue of the ζ Series Convergence and Loop Corrections in the Generation of Observable Primordial Non-Gaussianity in Slow-Roll Inflation. Part I: the Bispectrum,” JCAP **0808**, 029 (2008) [arXiv:0806.1546 [astro-ph]];

- Y. Rodriguez and C. A. Valenzuela-Toledo, “On the Issue of the ζ Series Convergence and Loop Corrections in the Generation of Observable Primordial Non-Gaussianity in Slow-Roll Inflation. Part II: the Trispectrum,” *Phys. Rev. D* **81**, 023531 (2010) [arXiv:0811.4092 [astro-ph]].
- [25] X. Gao and B. Hu, “Primordial Trispectrum from Entropy Perturbations in Multifield DBI Model,” arXiv:0903.1920 [astro-ph.CO].
- [26] S. Mizuno, F. Arroja, K. Koyama and T. Tanaka, “Lorentz boost and non-Gaussianity in multi-field DBI-inflation,” arXiv:0905.4557 [hep-th].
- [27] X. Gao, M. Li and C. Lin, “Primordial Non-Gaussianities from the Trispectra in Multiple Field Inflationary Models,” arXiv:0906.1345 [astro-ph.CO].
- [28] S. Mizuno, F. Arroja and K. Koyama, “On the full trispectrum in multi-field DBI inflation,” arXiv:0907.2439 [hep-th].
- [29] P. Adshead, R. Easther and E. A. Lim, “The ‘in-in’ Formalism and Cosmological Perturbations,” arXiv:0904.4207 [hep-th].
- [30] N. Kogo and E. Komatsu, “Angular Trispectrum of CMB Temperature Anisotropy from Primordial Non-Gaussianity with the Full Radiation Transfer Function,” *Phys. Rev. D* **73**, 083007
- [31] D. Jeong and E. Komatsu, “Primordial non-Gaussianity, scale-dependent bias, and the bispectrum of galaxies,” arXiv:0904.0497 [astro-ph.CO].
- [32] V. Desjacques and U. Seljak, “Signature of primordial non-Gaussianity of ϕ^3 -type in the mass function and bias of dark matter haloes,” arXiv:0907.2257 [astro-ph.CO].
- [33] P. Chingangbam and C. Park, “Statistical nature of non-Gaussianity from cubic order primordial perturbations: CMB map simulations and genus statistic,” arXiv:0908.1696 [astro-ph.CO].
- [34] P. Vielva and J. L. Sanz, “Constraints on fnl and gnl from the analysis of the N-pdf of the CMB large scale anisotropies,” arXiv:0910.3196 [astro-ph.CO].
- [35] M. Maggiore and A. Riotto, “The Halo Mass Function from Excursion Set Theory with a Non-Gaussian Trispectrum,” arXiv:0910.5125 [astro-ph.CO].
- [36] K. Izumi and S. Mukohyama, “Trispectrum from Ghost Inflation,” arXiv:1004.1776 [hep-th].

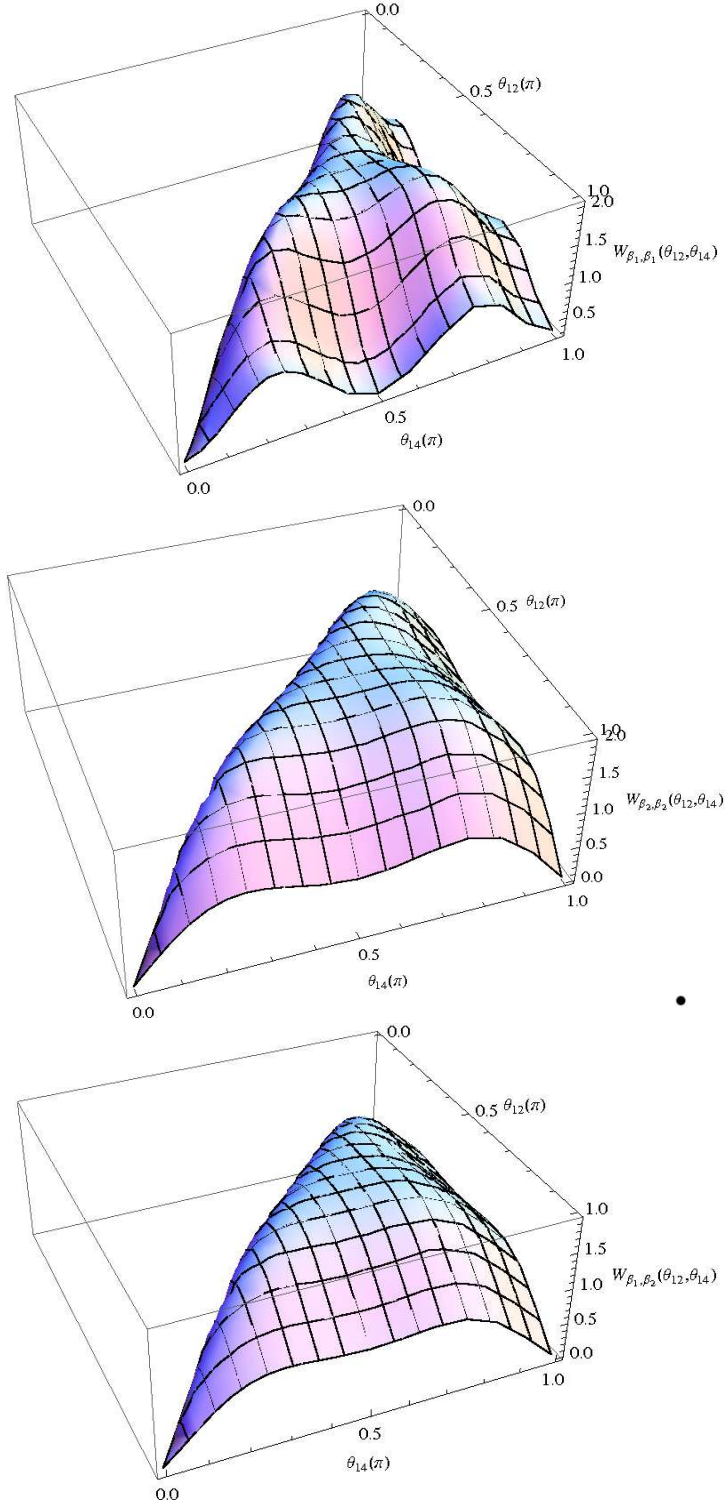


Figure 8: The functions $W_{\beta_1, \beta_1}(\theta_{12}, \theta_{14})$, $W_{\beta_2, \beta_2}(\theta_{12}, \theta_{14})$ and $W_{\beta_1, \beta_2}(\theta_{12}, \theta_{14})$.